Letter

Discovery of an Orally Bioavailable Dual PI3K/mTOR Inhibitor Based on Sulfonyl Substituted Morpholinopyrimidines

Sida Shen, Xiangyu He, Zheng Yang, Liang Zhang, Yingtao Liu, Zhiyuan Zhang, Weiwei Wang, Wei Liu, Yufeng Li, Dong Huang, Kai Sun, Xiaojing Ni, Xu Yang, Xinxin Chu, Yumin Cui, Qiang Lv, Jiong Lan, and Fusheng Zhou

ACS Med. Chem. Lett., **Just Accepted Manuscript** • DOI: 10.1021/acsmedchemlett.8b00167 • Publication Date (Web): 25 Jun 2018

Discovery of an Orally Bioavailable Dual PI3K/mTOR Inhibitor Based on Sulfonyl Substituted Morpholinopyrimidines

Sida Shen, Xiangyu He, Zheng Yang, Liang Zhang, Yingtao Liu, Zhiyuan Zhang, Weiwei Wang, Wei Liu, Yufeng Li, Dong Huang, Kai Sun, Xiaojing Ni, Xu Yang, Xinxin Chu, Yumin Cui, Qiang Lv, Jiong Lan, Fusheng Zhou*

Yangtze River Pharmaceutical Group, Shanghai Haiyan Pharmaceutical Technology Co. Ltd., No. 8, 67 Libing Road, Shanghai 201203, China

KEYWORDS: phosphoinositide-3-kinase, mammalian target of rapamycin, dual PI3K/mTOR inhibitor, morpholino-pyrimidine.

ABSTRACT: The discovery and optimization of a series of 2-morpholino-pyrimidine derivatives containing various sulfonyl side chains at the C_4 position led to the identification of compound **26** as a potent dual PI3K/mTOR inhibitor. It exhibited high inhibitory activity against PI3Kα/β/γ/δ (IC_{50} = 20/376/204/46 nM), mTOR (IC_{50} = 189 nM), potent functional suppression of AKT phosphorylation (IC_{50} = 196 nM), and excellent anti-proliferative effects on a panel of cancer cells. Enzymic data and modeling simulation indicate that cyclopropyl ring on the C_4 sulfone chain and fluorine on the C_6 aminopyridyl moiety are responsible for its maintained PI3K activity and enhanced mTOR potency, respectively. Furthermore, compound **26** exhibited higher efficiency in the HT-29 colorectal carcinoma xenograft model at the daily dose of 3.75 mg/kg and 7.5 mg/kg relative to **BKM120** at the dose of 15 mg/kg and 30 mg/kg.

The phosphatidylinositol 3-kinase (PI3K)-protein kinase B (AKT)-mammalian target of rapamycin (mTOR) transduction pathway plays a critical role in a diverse set of cellular functions, including cell growth, proliferation, motility, differentiation, and survival, which is often constitutively dysregulated in various human cancers, providing validated therapeutic targets associated with a wide range of human malignancies.[1] PI3Ks can be divided into class I, II, and III according to their structural characteristics and substrate preferences.[2] The most studied class I PI3K is a heterodimer protein that is composed of a catalytic subunit (p110α, p110β, p110δ, and p110γ) and a regulatory subunit (p85, p101, or p87).[3] The p110 catalytic subunits are able to convert phosphatidylinositol diphosphate (PIP2) to phosphatidylinositol triphosphate (PIP3), which leads to the subsequent activation of serine-threonine kinase AKT in terms of phosphorylation of AKT.[4] The downstream kinase mTOR, a central regulator of cell growth and proliferation, can be further activated by phosphorylated AKT (pAKT).[5] Compared with individually targeting PI3K or mTOR, dual inhibition of PI3K and mTOR has recently been proposed to represent a more effective approach for cancer therapy, since this strategy can directly target the most commonly mutated kinase-PI3K (which is generally encoded by the gene *PIK3CA* in the catalytic site of the p110α subtype[6]) while overcoming multiple mTOR-related negative feedback loops that a selective mTOR inhibitor usually fails to repress.[7]

NVP-BKM120 (**BKM**, Figure 1), a compound with a pyrimidine scaffold developed by Novartis AG, displayed a potent and selective class I PI3K inhibition over many other related kinases and is undergoing phase III clinical trials for breast cancer treatment (NCT01572727, NCT01610284, and NCT01633060).[8, 9] The C_6 aminopyridyl moiety on **BKM** interacts *via* hydrogen bonding with Asp836, Asp841, and Tyr867 and the 2-morpholine oxygen forms an important hydrogen bond to the hinge Val882 NH that is considered as an identical group for PI3K potency (Figure 1).[8] A variety of structural modification have been done focused on the replacement of its pyrimidine core scaffold and C_6 aminopyridyl moiety with different bicyclic cores and aromatic urea/indole side chains, respectively, and anilines and aminoheterocycles are predominant substitutions at the core pyrimidine C_4 position that orient towards solvent without any specific hydrogen bonding.[8, 10-12] The discovery of morpholinopyrimidine based selective mTOR inhibitor **AZD3147** from Astra Zeneca indicates that the NH groups on C_6 phenylthiourea or indole side chain are critical to engage productive interactions with glutamic acid present in mTOR but not PI3K, while C_4 sulfonyl side chains do not participate any specific interaction (Figure 1).[13, 14, 15] Thus, C_4 positions at the core pyrimidine of both mTOR inhibitors and PI3K inhibitors can consider as flexible sites for generating new ligands with druggable properties and retained potency where are capable to tolerate a range of substituents.

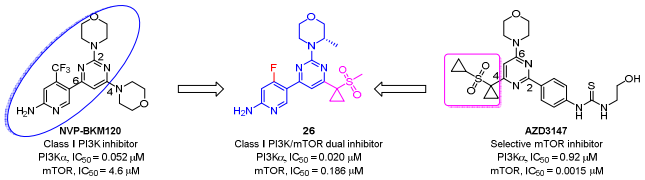

Figure 1. The design of a novel PI3K/mTOR dual inhibitor **26**.

Herein, we describe a hybridization approach to discover novel morpholinopyrimidines based PI3K inhibitors by replacing the C_4 morpholine moiety on the **BKM** with sulfonyl portion taken from the selective mTOR inhibitors. Structure-activity relationship (SAR) studies conducted on twenty-seven new analogs lead to the identification of compound **26** (Figure 1), a potent dual inhibitor of PI3K and mTOR that exhibits remarkable cellular anti-proliferative effects compared to **BKM**. Enzymic data and modeling simulation fully explain that cyclopropyl ring on the C_4 sulfone chain and fluorine on the C_6 aminopyridyl moiety are responsible for its maintained PI3K activity and enhanced mTOR potency, respectively. Furthermore, compound **26** also exhibits encouraging ADMET properties and significant *in vivo* tumor growth inhibitory efficacy in the HT-29 colorectal carcinoma xenograft mouse model compared to **BKM**.

The structural modifications were focused on the sulfonyl side chains with different substituents on the methylene unit and the terminal area. The detailed synthetic procedures and spectrum data of final products **1-27** are provided in supporting information (Scheme S1). all the new analogs were initially evaluated for *in vitro* activities by testing PI3Kα enzymic inhibition, the resulting suppression of pAKT in PC-3 cells, and subsequent antiproliferation assays on breast cancer cell lines T47D and MCF-7 carrying a *PIK3CA* H1047R mutation and E545K mutation, respectively (Table 1).[16] The exploration of alkylation or fluorination at the methylene unit of the sulfone portion led to an improvement in potency in most cases (entries **1-9**), whereas these trends weren't observed in isopropyl (**4**) and cyclohexyl (**9**) analogs indicating a limit to the size of the substituent. Among these analogs, the IC_{50} values of the *gem*-dimethyl (**5**), cyclopropyl (**6**), and cyclobutyl (**7**) analogs were lower than 20 nM against PI3Kα, accompanied by an improvement in cellular phosphorylation of AKT and antiproliferation in comparison with the reference compound **BKM**. The replacement of morpholine with (*R*)-3-methylmorpholine (in compound **10**) resulted in a 14-fold decrease in activity relative to the parent compound **6**. In the meanwhile, the (*S*)-3-methylmorpholine analog **11** maintained enzymic and cellular effects comparable to those of **6**. Further exploration of the (*S*)-3-methylmorpholine fragment paired with *gem*-dimethyl, cyclobutyl, and cyclopentyl substituents adjacent to the sulfone side chain (in compounds **12-14**) turned out a consistent 2-fold enhancement in enzymic potency. Moreover, this optimization identified compound **13** with low IC_{50} values of 93 nM and 78 nM against T47D and MCF-7 in MTT cell proliferation assays, respectively. Another selection of analogs was made to explore replacement of the terminal methyl group of the sulfone with ethyl, isopropyl, and phenyl groups (entries **15-23**). The ethyl and isopropyl terminal groups did not lead to better activity (compounds **15-18**), even though they were combined with the favorable cyclopropyl or *gem*-dimethyl sulfonyl moieties. Compound **20** featuring a terminal phenyl group combined with *gem*-dimethyl showed low nanomolar activity against PI3Kα, but it was relatively weak in the cellular assessment. Interestingly, cellular potency was significantly enhanced once one extra fluorine atom was located at the ortho-position of phenyl ring adjacent to the sulfone (compound **23**). Replacement of the trifluoromethyl substituent on the aminopyridyl moiety with fluorine led to a slightly decrease in potency against PI3Kα, however the anti-proliferative effects of the resulting compounds **24-27** were dramatically elevated, especially in the (*S*)-3-methylmorpholine based analogs **26** and **27**, which were found to be 10 times more active than **BKM** against T47D and MCF-7 cells. Additionally, good corrections were observed between cellular p-AKT inhibition in PC-3 cells and antiproliferation results in T47D (R^2 = 0.88) and MCF-7 cells (R^2 = 0.92) (Figure S1) which demonstrates that p-AKT inhibition is responsible for the cellular anti-proliferative effects even if in the different cells. Nevertheless, 2D plot of biochemical PI3Kα activity and cellular p-AKT inhibition doesn't show a nice linear regression (R^2 = 0.53) that may be related to distinct permeability.

Table 1. Structure−Activity Relationship Studies at the R^1, R^2, and R^3 Groups.[a]

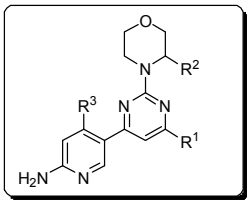

Compound	R^1	R^2	R^3	PI3Kα IC_{50} (μM)	PC-3 pAKT IC_{50} (μM)	T47D IC_{50} (μM)	MCF-7 IC_{50} (μM)
1		H	CF_3	0.189	3.01	1.668	1.513
2		H	CF_3	0.056	2.446	1.155	1.139
3		H	CF_3	0.025	0.846	0.513	0.408
4		H	CF_3	0.218	n/d[b]	n/d	n/d
5		H	CF_3	0.013	0.312	0.058	0.224
6		H	CF_3	0.013	0.319	0.167	0.283

7		H	CF_3	0.015	0.248	0.138	0.134
8		H	CF_3	0.042	0.384	0.218	0.34
9		H	CF_3	0.321	n/d	n/d	n/d
10		(*R*)-CH_3	CF_3	0.223	n/d	n/d	n/d
11		(*S*)-CH_3	CF_3	0.009	0.546	0.129	0.112
12		(*S*)-CH_3	CF_3	0.006	0.306	0.175	0.214
13		(*S*)-CH_3	CF_3	0.006	0.184	0.093	0.078
14		(*S*)-CH_3	CF_3	0.022	0.674	0.139	0.159
15		H	CF_3	0.013	0.301	0.225	0.295
16		H	CF_3	0.040	0.947	0.552	0.512
17		H	CF_3	0.058	0.43	0.16	0.437
18		H	CF_3	0.065	1.178	1.063	0.599
19		H	CF_3	0.026	0.668	0.324	0.513
20		H	CF_3	0.009	1.548	0.478	0.897
21	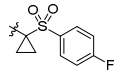	H	CF_3	0.057	1.275	0.619	0.5715
22	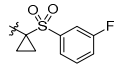	H	CF_3	0.014	0.606	0.242	0.286
23		H	CF_3	0.007	0.367	0.129	0.184
24		H	F	0.041	0.369	0.062	0.027
25		H	F	0.066	0.215	0.123	0.104
26		(*S*)-CH_3	F	0.010	0.196	0.03	0.011
27		(*S*)-CH_3	F	0.020	0.121	0.033	0.015
BKM	-	-		0.041	0.365	0.286	0.206

[a]IC_{50}, the mean value of duplicate measurements; [b]n/d: not determined.

Compounds **1**, **6**, **11**, and **26** were selected for further characterization in other three class I PI3K subtypes as well as mTOR. The results shown in Table 2 indicate cyclopropyl ring presented on the sulfone chain plays important role to maintain comparable Class I PI3K relative to **BKM**. Notably, converting the trifluoromethyl group (**11**) to fluorine (**26**) on the C_6 aminopyridyl moiety led to a 11-fold potency increase against mTOR and 4-fold improved potency at PI3Kδ subtypes. As the sulfone side chain is also present in inhibitors of Ataxia telangiectasia mutated and RAD3-related (ATR) belonging to phosphatidylinositol 3-kinase-related kinase (PIKK) family,[17] the capability of compounds **1**, **6**, **11**, and **26** to impact the ATR cellular activity in terms of inhibition of phosphorylation of Chk1 Ser-345 were also evaluated in HT-29 cells. **1**, **6**, **11**, and **BKM** were found to be inactive up to 10 μM, while **26** shows slight inhibition at the concentration of 10 μM (Figure 2).

Table 2. Class I PI3K and mTOR inhibitory activities of compounds **1**, **6**, **11**, and **26**.[a]

Compound	Enzyme IC_{50} (μM)				
	PI3Kα	**PI3Kβ**	**PI3Kγ**	**PI3Kδ**	**mTOR**

1	0.189	n/d[b]	n/d	n/d	13.98
6	0.016	0.314	0.288	0.240	1.680
11	0.016	0.264	0.164	0.197	2.120
26	0.020	0.376	0.204	0.046	0.186
BKM	0.040	0.234	0.372	0.125	1.981

[a]IC_{50}, the mean values of duplicate measurements. [b] n/d: not determined.

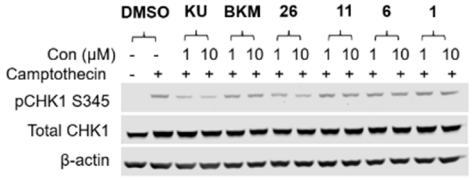

Figure 2. Effect of compounds **1**, **6**, **11**, and **26** on ATR activity in the presence of DNA damage. HT-29 were pre-treated with indicated compounds for 1 h, DNA damage was induced by exposure to camptothecin. ATR activity was measured by detecting phosphorylation of substrate Chk1, total Chk1 and β-actin were shown as internal control. KU-60019 (KU) is a specific inhibitor of ATM/ATR and DNA-PK.

Thirteen potent compounds (**3**, **5-7**, **13**, **16**, **18**, **20**, **23-27**) were used for metabolic stability study in human and mouse liver microsomes to identify metabolically stable compounds for *in vivo* studies. The results shown in Table S1 indicate that the compounds containing trifluoromethyls exhibit a significantly low metabolic stability relative to **BKM** (Cl_{int}: human, 10.86 mL/min/kg; mouse, 151.33 mL/min/kg) except the compound **6** (Cl_{int}: human, 9.86 mL/min/kg; mouse, 185.15 mL/min/kg). A cyclobutane ring on the methylene unit, a (*S*)-3-methylmorpholine moiety, and an aromatic terminal groups are particularly detrimental to metabolic stability in this series. However, aminofluoropyridines **24-27** exhibited comparable or much better liver microsomal stability both in human (Cl_{int}: 5-16 mL/min/kg) and mouse (Cl_{int}: 40-140 mL/min/kg) in comparison with **BKM**. Given its enhanced mTOR potency and metabolic stability, we were interested in advancing compound **26** into more characterization.

A panel of cell lines was chosen to carry out antiproliferation screening to compare **26** and **BKM**. The treatment of **26** turned out 2.5-fold to 18.7-fold improvement against different cells (Figure 3A, Table S2), while stronger cytotoxicity against HUVECs (**26**, IC_{50} = 0.108 μM; **BKM**, IC_{50} = 0.886 μM) was also observed without certain cell selectivity. It is known that **BKM** shows effects on the destabilization of microtubule that contributes to its therapeutic intervention together with its PI3K inhibition.[18] we thought that this property might transfer to the new hybrid analogs due to their structural similarity. A dose-response cell cycle study in HT-29 cell showed **BKM** accumulated cells dominantly in G2/M fraction as expected that leads to mitotic arrest or apoptosis (Figure 3C). In contrast, the treatment of **26** arrested cells in the G1 fraction which acts same as cytostatics (Figure 3B). In addition, no obvious effect of **26** at 10 μM concentration was observed in an off-target test containing twenty-eight different kinases (Table S3) and **26** exhibited comparable results with **BKM** against the mutant PI3Kα E542K, E545K, H1047R subtype inhibition. Overall, the experimental results elucidate that the elevated mTOR activity is responsible for its dramatically improved cellular anti-proliferative effects.

To better understand the interactions with targeted proteins, docking simulations were performed for compound **26** with PI3Kα, mTOR, and tubulin (Figure 4)**.** The binding mode of **26** to PI3Kα is very similar to that of **BKM**, which is responsible for similar potency against PI3Kα. The morpholine forms a key hydrogen bond with Val851 (Val2240 on mTOR) in the hinge region, the amino group at the 2-position of the pyridine engages in another hydrogen bond with Asp810 (Asp2195 on mTOR), the sulfone side chain occupies the ribose pocket, and the fluorine at the 4-position of the pyridine is involved in an attractive electrostatic interaction with Lys802. At the same position on mTOR, the residue is Glu2190 which causes a repulsive force that twists the binding of compound **26** and thereby enhances the compound's potency at mTOR. Moreover, the overlapped docking poses with tubulin indicate that cyclopropyl group of **26** is too big to accommodate the tubulin binding site due to the steric hindrance with Lys352, leading to a binding displacement from **BKM** and weaker binding to tubulin, which may differentiate **26** with **BKM**.

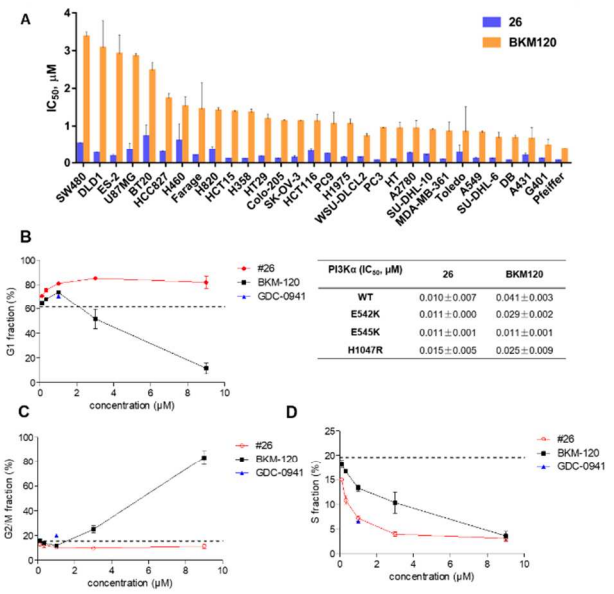

Figure 3. PI3Kα mutant enzymic data, cancer cell panel screening (A), and cell cycle distribution in HT-29 cells (B-D) of **26**.

Further ADMET profiling demonstrates compound **26** does not inhibit the most common cytochrome P_{450} enzymes (CYP) 1A2, 2B6, 2C8, 2C9, 2C19, 2D6, and 3A4 (IC_{50} values > 10 μM, Table S4). *In vitro* evaluation on human hERG channel current indicated a minimal risk of 26 induced long QT syndrome (IC_{50} > 30 μM, Figure S2). The Caco-2 permeability assay determined **26** as a high permeable compound on both sides (P_{app} >10 × 10^{-6} cm/s) with favorable efflux ratio (P_{app} (B-A)/ P_{app} (A-B) = 0.66, Table S5), which is supportive for its excellent cellular potency. A pharmacokinetic (PK) profiling was further performed for compound **26** in CD1 mice. As presented in Figure 5 (left), intravenous administration of **26** to mice at 5 mg/kg (dissolved in 15% Captisol) exhibited a similar clearance rate (15.2 mL/min/kg), volume of distribution (1.40 L/kg), and half-life (1.59 h) relative to the corresponding parameters of **BKM** disclosed in the literature.[8] Oral admin-

istration to mice at 10 mg/kg (dissolved in 15% Captisol) yielded a high C_{max} (2984 ng/mL) and plasma exposure (AUC_{last} = 10379 h*ng/mL) with an excellent oral bioavailability (F% = 94.6%).

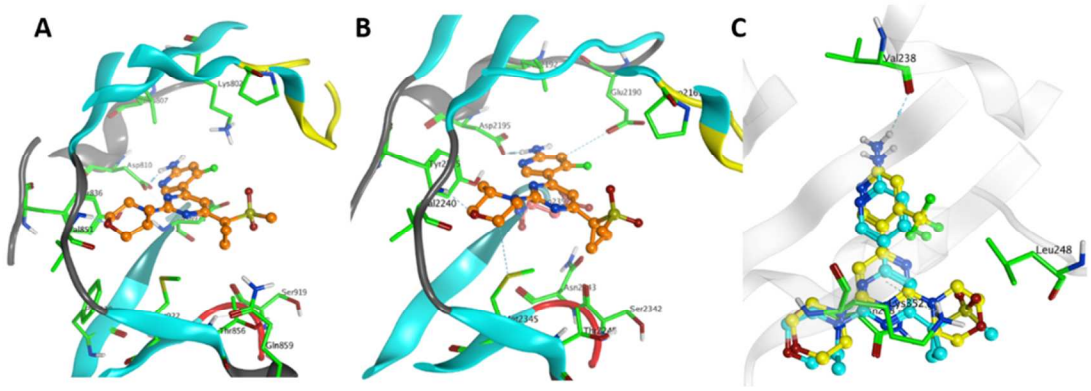

Figure 4. Docking poses of **26** (orange) with PI3Kα (A, PDB entry: 4l23), mTOR (B, PDB entry: 4jt6), and tubulin (C, **26**: cyan, **BKM**: yellow, entry: 5m7e).

i.v. (mouse) at 5 mg/kg				
Cl	V_{ss}	$T_{1/2}$	AUC_{last}	
(mL/min/kg)	(L/kg)	(hr)	(hr*ng/mL)	
15.2	1.4	1.4	5435	
p.o. (mouse) at 10 mg/kg				
C_{max}	T_{max}	$T_{1/2}$	AUC_{last}	F%
(ng/mL)	(hr)	(hr)	(hr*ng/mL)	
2984	0.25	2.87	10397	94.6%

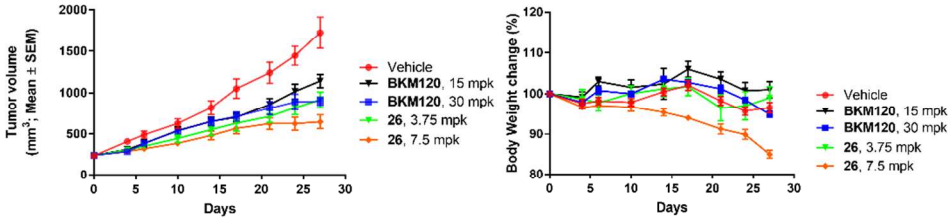

Figure 5. PK parameters and efficacy studies of **26**. (*left*) Male CD1 mice (n =18) were assigned to 2 groups: 9 animals were administered via oral gavage (10 mg/kg) and 9 animals were administrated via tail vein injection (5 mg/kg). Blood samples were collected at 0.083, 0.25, 0.5, 1, 2, 4, 8 and 24 h post dose (n = 3 mice per time point). (*middle*) Balb/c *nu/nu* mice bearing HT-29 xenograft tumors were treated with vehicle, **BKM** (15 or 30 mg/kg), or **26** (3.75 or 7.5 mg/kg) by daily oral gavage for 27 days when the mean tumor size was around 240 mm^3. The estimated tumor volume was plotted versus time. The tumor growth inhibition (TGI) was calculated after 27-day treatment (**26**, 3.75 mpk, TGI = 54.4%, **p* = 0.02; **26**, 7.5 mpk, TGI = 72.9%, **p* = 0.02; **BKM**, 15 mpk, TGI = 39.4%, **p* = 0.02; **BKM**, 30 mpk, TGI = 55.7%, **p* = 0.04). (*right*) The body weight change (BWC) was measured, calculated and plotted versus time. All data are presented as the mean ± SEM (n = 6). Dunnett's multiple comparison test. *<0.05.

With these encouraging *in vitro* effects and preliminary ADMET profiling, compound **26** was tested in *in vivo* efficacy studies in the end. HT-29 colorectal carcinoma xenograft mouse model carrying the *PIK3CA* P449T mutation was selected for our efficacy studies, as the PI3K/AKT/mTOR pathway is being considered as a potential therapeutic target for the treatment of colorectal cancer.[19] Considering the higher cytotoxicity and stronger anti-proliferative effects of **26**, 4-fold lower doses (3.75 and 7.5 mg/kg) were selected in comparison with **BKM** at the doses of 15 and 30 mg/kg, respectively (Figure 5, middle). **BKM** only produced 39.4% tumor growth inhibition (TGI) with the treatment of 15 mg/kg, while better single agent efficacy (TGI = 54.4%) was observed with **26** at daily oral doses of 3.75 mg/kg for 27 days in a well-tolerated manner, which was comparable to the result with **BKM** at the dose of 30 mg/kg (TGI = 55.7%). Interestingly, the proliferation assay result of **BKM** (IC_{50} = 1.186 μM) in HT-29 cell was also about 7.3 folds higher than **26** (IC_{50} = 0.163 μM) (Table S2) which suggests a hint of correlation between *in vivo* tumor suppression and *in vitro* anti-proliferation activity, although drug exposure in tumor tissue and *in vivo* target modulation haven't been determined. The 7.5 mg/kg group of **26** displayed more significant TGI (72.9%) All animals were survival after 27-day treatment, whereas 15% weigh loss was observed in **26** 7.5 mg/kg group (Figure 5, right). Notably, 60 mg/kg **BKM** was also enrolled at the beginning of in this study that was terminated after 10-day treatment due to serious toxicity (weigh loss >25%, Figure S3).

In summary, we have designed and synthesized a new series of 6-aminopyridyl, 4-sulfonyl, 2-morpholino-pyrimidine core analogs as novel PI3K inhibitors. Through the SAR profiling of different substituents at the methylene unit and the terminal region of sulfonyl side chains, as well as the combination with different morpholino and aminopyridyl moieties, we successfully addressed the identification of orally bioavailable compound **26**, which exhibited potent enzymic activity against Class I PI3K and PI3Kα mutant isoforms, improved mTOR potency, good suppression of pAKT in cellular assays, and promising pharmacokinetic parameters. Significantly, compound **26** was found to be much more effective both in *in vitro* and *in vivo* studies compared to **BKM**.

ASSOCIATED CONTENT

Supporting Information

The Supporting Information is available free of charge on the ACS Publications website.

Supplementary figures and table, details of the synthetic chemistry, docking studies, and biological assays (PDF)

AUTHOR INFORMATION

Corresponding Author

F. Z.: email: fushengz@haiyanpharma.com, zhoufs2015@163.com.

ORCID

Fusheng Zhou: 0000-0002-6277-906X;

Sida Shen: 0000-0002-0295-2545.

Author Contributions

The manuscript was written through contributions of all authors. All authors have given approval to the final version of the manuscript.

Funding Sources

The work was sponsored by Shanghai Rising-star Program 17QB401100.

ABBREVIATIONS

PI3K: phosphatidylinositol 3-kinase; AKT: protein kinase B; mTOR: mammalian target of rapamycin; PIP2: phosphatidylinositol diphosphate; PIP3: phosphatidylinositol triphosphate; pAKT: phosphorylated AKT; ADMET: absorption, distribution, metabolism, excretion, and toxicity; SAR: structure-activity relationship; PK: pharmacokinetics; AUC: area under curve; CYP: cytochrome P450; hERG: human *ether-a-go-go*-related gene; i.v.: intravenous administration; p.o.: oral administration; TGI: tumor growth inhibition.

REFERENCES

1. Engelman, J. A., Targeting PI3K signalling in cancer: opportunities, challenges and limitations. *Nat. Rev. Cancer* **2009,** *9*, 550-62.
2. Katso, R.; Okkenhaug, K.; Ahmadi, K.; White, S.; Timms, J.; Waterfield, M. D., Cellular function of phosphoinositide 3-kinases: implications for development, homeostasis, and cancer. *Annu. Rev. Cell Dev. Bio.* **2001,** *17*, 615-75.
3. Thorpe, L. M.; Yuzugullu, H.; Zhao, J. J., PI3K in cancer: divergent roles of isoforms, modes of activation and therapeutic targeting. *Nat. Rev. Cancer* **2015,** *15*, 7-24.
4. Manning, B. D.; Cantley, L. C., AKT/PKB signaling: navigating downstream. *Cell* **2007,** *129*, 1261-74.
5. Guertin, D. A.; Sabatini, D. M., Defining the role of mTOR in cancer. *Cancer Cell* **2007,** *12*, 9-22.
6. Samuels, Y.; Wang, Z.; Bardelli, A.; Silliman, N.; Ptak, J.; Szabo, S.; Yan, H.; Gazdar, A.; Powell, S. M.; Riggins, G. J.; Willson, J. K.; Markowitz, S.; Kinzler, K. W.; Vogelstein, B.; Velculescu, V. E., High frequency of mutations of the PIK3CA gene in human cancers. *Science* **2004,** *304*, 554.
7. Fan, Q. W.; Knight, Z. A.; Goldenberg, D. D.; Yu, W.; Mostov, K. E.; Stokoe, D.; Shokat, K. M.; Weiss, W. A., A dual PI3 kinase/mTOR inhibitor reveals emergent efficacy in glioma. *Cancer Cell* **2006,** *9*, 341-9.
8. Burger, M. T.; Pecchi, S.; Wagman, A.; Ni, Z. J.; Knapp, M.; Hendrickson, T.; Atallah, G.; Pfister, K.; Zhang, Y.; Bartulis, S.; Frazier, K.; Ng, S.; Smith, A.; Verhagen, J.; Haznedar, J.; Huh, K.; Iwanowicz, E.; Xin, X.; Menezes, D.; Merritt, H.; Lee, I.; Wiesmann, M.; Kaufman, S.; Crawford, K.; Chin, M.; Bussiere, D.; Shoemaker, K.; Zaror, I.; Maira, S. M.; Voliva, C. F., Identification of NVP-BKM120 as a Potent, Selective, Orally Bioavailable Class I PI3 Kinase Inhibitor for Treating Cancer. *ACS Med. Chem. Lett.* **2011,** *2*, 774-9.
9. Maira, S. M.; Pecchi, S.; Huang, A.; Burger, M.; Knapp, M.; Sterker, D.; Schnell, C.; Guthy, D.; Nagel, T.; Wiesmann, M.; Brachmann, S.; Fritsch, C.; Dorsch, M.; Chene, P.; Shoemaker, K.; De Pover, A.; Menezes, D.; Martiny-Baron, G.; Fabbro, D.; Wilson, C. J.; Schlegel, R.; Hofmann, F.; Garcia-Echeverria, C.; Sellers, W. R.; Voliva, C. F., Identification and characterization of NVP-BKM120, an orally available pan-class I PI3-kinase inhibitor. *Mol. Cancer Ther.* **2012,** *11*, 317-28.
10. Andrs, M.; Korabecny, J.; Jun, D.; Hodny, Z.; Bartek, J.; Kuca, K., Phosphatidylinositol 3-Kinase (PI3K) and phosphatidylinositol 3-kinase-related kinase (PIKK) inhibitors: importance of the morpholine ring. *J. Med. Chem.* **2015,** *58*, 41-71.
11. Zhang, J. Q.; Luo, Y. J.; Xiong, Y. S.; Yu, Y.; Tu, Z. C.; Long, Z. J.; Lai, X. J.; Chen, H. X.; Luo, Y.; Weng, J.; Lu, G., Design, Synthesis, and Biological Evaluation of Substituted Pyrimidines as Potential Phosphatidylinositol 3-Kinase (PI3K) Inhibitors. *J. Med. Chem.* **2016,** *59*, 7268-74.
12. Burger, M. T.; Knapp, M.; Wagman, A.; Ni, Z. J.; Hendrickson, T.; Atallah, G.; Zhang, Y.; Frazier, K.; Verhagen, J.; Pfister, K.; Ng, S.; Smith, A.; Bartulis, S.; Merrit, H.; Weismann, M.; Xin, X.; Haznedar, J.; Voliva, C. F.; Iwanowicz, E.; Pecchi, S., Synthesis and in Vitro and in Vivo Evaluation of Phosphoinositide-3-kinase Inhibitors. *ACS medicinal chemistry letters* **2011,** *2*, 34-8.
13. Finlay, M. R.; Buttar, D.; Critchlow, S. E.; Dishington, A. P.; Fillery, S. M.; Fisher, E.; Glossop, S. C.; Graham, M. A.; Johnson, T.; Lamont, G. M.; Mutton, S.; Perkins, P.; Pike, K. G.; Slater, A. M., Sulfonyl-morpholino-pyrimidines: SAR and development of a novel class of selective mTOR kinase inhibitor. *Bioorganic Med. Chem. Lett.* **2012,** *22*, 4163-8.
14. Pike, K. G.; Morris, J.; Ruston, L.; Pass, S. L.; Greenwood, R.; Williams, E. J.; Demeritt, J.; Culshaw, J. D.; Gill, K.; Pass, M.; Finlay, M. R.; Good, C. J.; Roberts, C. A.; Currie, G. S.; Blades, K.; Eden, J. M.; Pearson, S. E., Discovery of AZD3147: a potent, selective dual inhibitor of mTORC1 and mTORC2. *ACS Med. Chem. Lett.* **2015,** *58*, 2326-49.
15. Morris, J. J.; Pike, K. G. Trisubstituted pyrimidine derivatives for the treatment of proliferative disease. *WO 2009007748 A2*.
16. O'Brien, C.; Wallin, J. J.; Sampath, D.; GuhaThakurta, D.; Savage, H.; Punnoose, E. A.; Guan, J.; Berry, L.; Prior, W. W.; Amler, L. C.; Belvin, M.; Friedman, L. S.; Lackner, M. R., Predictive biomarkers of sensitivity to the phosphatidylinositol 3' kinase inhibitor GDC-0941 in breast cancer preclinical models. *Clin. Cancer Res.* **2010,** *16*, 3670-83.
17. Foote, K. M.; Blades, K.; Cronin, A.; Fillery, S.; Guichard, S. S.; Hassall, L.; Hickson, I.; Jacq, X.; Jewsbury, P. J.; McGuire, T. M.; Nissink, J. W.; Odedra, R.; Page, K.; Perkins, P.; Suleman, A.; Tam, K.; Thommes, P.; Broadhurst, R.; Wood, C., Discovery of 4-{4-[(3R)-3-Methylmorpholin-4-yl]-6-[1-(methylsulfonyl)cyclopropyl]pyrimidin-2-yl}-1H-indole (AZ20): a potent and selective inhibitor of ATR protein kinase with monotherapy in vivo antitumor activity. *J. Med. Chem.* **2013,** *56*, 2125-38.
18. Bohnacker, T.; Prota, A. E.; Beaufils, F.; Burke, J. E.; Melone, A.; Inglis, A. J.; Rageot, D.; Sele, A. M.; Cmiljanovic, V.; Cmiljanovic, N.; Bargsten, K.; Aher, A.; Akhmanova, A.; Diaz, J. F.; Fabbro, D.; Zvelebil, M.; Williams, R. L.; Steinmetz, M. O.; Wymann, M. P., Deconvolution of Buparlisib's mechanism of action defines specific PI3K and tubulin inhibitors for therapeutic intervention. *Nature Comm.* **2017,** *8*, 14683.
19. Bahrami, A.; Khazaei, M.; Hasanzadeh, M.; ShahidSales, S.; Joudi Mashhad, M.; Farazestanian, M.; Sadeghnia, H. R.; Rezayi, M.; Maftouh, M.; Hassanian, S. M.; Avan, A., Therapeutic Potential of Targeting PI3K/AKT Pathway in Treatment of Colorectal Cancer: Rational and Progress. *J. Cell. Biochem.* **2018,** *119*, 2460-2469.

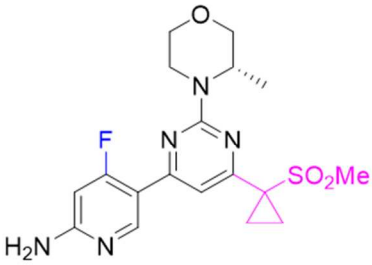

PI3K α-WT IC_{50} = 10 nM
PI3K α-E542K IC_{50} = 11 nM
PI3K α-E545K IC_{50} = 11 nM
PI3K α-H1047R IC_{50} = 15 nM
PI3K β IC_{50} = 376 nM
PI3K γ IC_{50} = 204 nM
PI3K δ IC_{50} = 46 nM
mTOR IC_{50} = 186 nM
F% = 94.9% (mouse)
TGI (HT-29) = 54.4% (3.75 mpk)
72.9% (7.5 mpk)